

## Structural Phase Transformation in the Cluster Chalcogenides $\text{EuMo}_6\text{S}_8$ and $\text{BaMo}_6\text{S}_8$

R. Baillif,<sup>(a)</sup> A. Dunand,<sup>(b)</sup> J. Muller,<sup>(a)</sup> and K. Yvon<sup>(b)</sup>

*Université de Genève, CH-1211 Genève 4, Switzerland*

(Received 15 June 1981)

Low-temperature x-ray-diffraction analysis at ambient pressure shows that the rhombohedral chalcogenides  $\text{EuMo}_6\text{S}_8$  and  $\text{BaMo}_6\text{S}_8$  transform at 110(5) and 175(10) K, respectively, into a triclinic distorted low-temperature structure. The transitions are presumably due to a Jahn-Teller-type electronic instability arising from the octahedral  $\text{Mo}_6$  clusters. The absence of superconductivity is attributed to the triclinic deformation of these clusters which leads to a significant splitting of the nearly half-filled Mo  $d$ -like conduction band.

PACS numbers: 64.70.Kb

The absence of superconductivity in Mo cluster chalcogenides  $M\text{Mo}_6X_8$  (where  $M$  denotes a metal, and  $X$  a chalcogen) containing divalent metal cations such as  $M=\text{Eu}^{2+}$  or the alkaline earths  $\text{Ca}^{2+}$ ,  $\text{Sr}^{2+}$ , and  $\text{Ba}^{2+}$  is surprising and, to our knowledge, has not been explained as yet.<sup>1</sup> According to self-consistent band-structure calculations performed by Jarlborg and Freeman,<sup>2</sup>  $\text{EuMo}_6\text{S}_8$  should be metallic and have a large density of states at  $E_F$ . Also, its superconducting transition temperature,  $T_c$ , should not be strongly depressed by the magnetic moment of the rare-earth ions  $\text{Eu}^{2+}$  because their interactions with the conduction electrons (mainly Mo  $d$ ) are small. Metallic behavior for  $\text{Eu}_{1.2}\text{Mo}_6\text{S}_8$  under hydrostatic pressure has been reported recently by Chu *et al.*,<sup>3</sup> who found this compound to become a high-temperature superconductor ( $T_c \sim 11$  K) at pressures above  $\sim 7$  kbar. This observation was also made by Harrison *et al.*,<sup>4</sup> who reported on pressure-induced superconductivity in pseudoternary  $\text{Sn}_x\text{Eu}_{1-x}\text{Mo}_6\text{S}_8$  compounds ( $0 \leq x \leq 0.1$ ), but surprisingly found semiconducting behavior at ambient pressure.

Several possible reasons for the absence of superconductivity at ambient pressure and the onset of high-temperature superconductivity at high pressure have been put forward and discussed by these authors.<sup>2-4</sup> Clearly, the arguments based on the magnetic character of the  $\text{Eu}^{2+}$  ions in  $\text{EuMo}_6\text{S}_8$  cannot be applied to compounds containing alkaline-earth ions such as  $\text{BaMo}_6\text{S}_8$ , which is also not superconducting above 1 K at ambient pressure. A possible explanation which has not been examined in much detail is the occurrence of a structural phase transition.

In this Letter we show that both compounds transform below room temperature and at ambient pressure into a triclinic distorted low-temperature structure. The transitions presumably have a common origin and are due to an electron-

ic instability of the octahedral  $\text{Mo}_6$  clusters.

Samples of composition  $\text{Eu}_{1.1}\text{Mo}_6\text{S}_8$  and  $\text{BaMo}_6\text{S}_8$  were prepared by heating mixtures of  $\text{EuS}$  (or  $\text{BaS}$ ), Mo, and S up to 1250°C for 24 h in evacuated and sealed quartz tubes. The reaction products were melted in a specially designed high-pressure furnace<sup>5</sup> at  $\sim 1800^\circ\text{C}$  under 2 kbar of 99.997% Ar, and were then analyzed by x-ray powder diffraction (Ni filtered  $\text{Cu } K\alpha$  radiation) on a commercially available goniometer (Philips PW 1050/25) which was equipped with a low-temperature continuous-He-flow cryostat (Thor Cryogenics Ltd.). The room-temperature patterns of  $\text{Eu}_{1.1}\text{Mo}_6\text{S}_8$  and  $\text{BaMo}_6\text{S}_8$  are shown in Figs. 1(a) and 2(a), respectively. Whereas for the Eu-based sample all lines could be indexed on the basis of the known rhombohedral cell of  $\text{EuMo}_6\text{S}_8$ ,<sup>1</sup> for the Ba-based sample several lines occurred in addition to those of rhombohedral  $\text{BaMo}_6\text{S}_8$  (Ref. 1) which belonged to  $\text{MoS}_2$  and a yet unknown phase. The lattice parameters of both compounds were refined from measured  $2\theta$  values of 25 reflections using Si as an internal standard. As shown in Table I, the cell volumes at 293 K are slightly larger than those published,<sup>1,3</sup> indicating that our compounds contained slightly more Ba and Eu, or were less S deficient than those examined previously by other authors.

The low-temperature patterns were recorded at  $\sim 10$  K. As can be seen in Figs. 1(b) and 2(b) they differ significantly from those obtained at room temperature. In particular, the rhombohedral reflections having sixfold multiplicity, such as  $10\bar{2}$  and  $1\bar{1}1$ , split into three nonequivalent reflections having twofold multiplicity, or showed considerable broadening, whereas those having twofold multiplicity, such as  $111$ , remain sharp. This indicates a triclinic deformation of the lattice and the occurrence of a structural phase transformation. A study of the line shape of the  $13\bar{1}$  reflection as a function of temperature showed

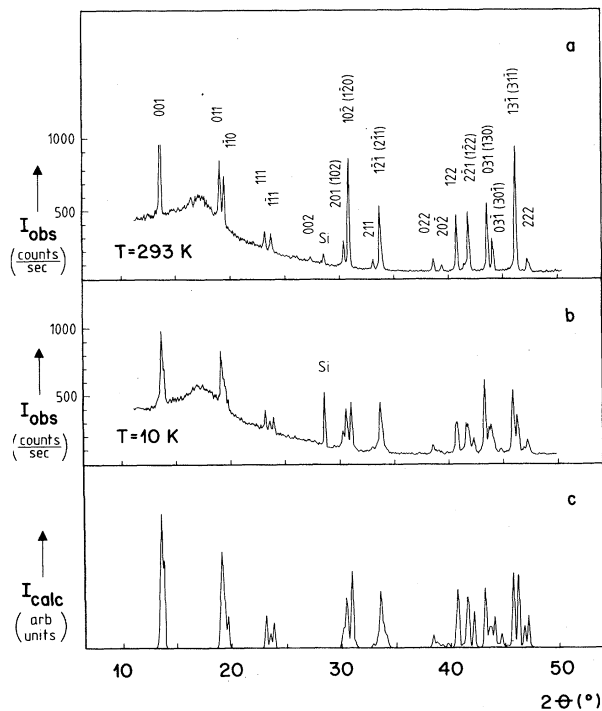


FIG. 1. The observed x-ray powder patterns of (a) the rhombohedral high-temperature phase, and (b) the triclinic low-temperature phase of  $\text{Eu}_{1-x}\text{Mo}_6\text{S}_8$ . The diffuse background peak at  $2\theta = 17^\circ$  is due to the sample holder. (c) The calculated powder pattern was simulated with LAZY PULVERIX (Ref. 6), assuming Gaussian line profiles of half width at half maximum of  $0.1 + 0.2 \tan\theta$  deg.

that the line splitting occurred quasidiscontinuously within a narrow temperature interval. For  $\text{EuMo}_6\text{S}_8$  it occurred at  $110 \pm 4$  K and for  $\text{BaMo}_6\text{S}_8$  at  $175 \pm 10$  K. The cell parameters of the triclinic low-temperature phases are reported in Table I. Clearly, the cell distortions are similar in both compounds, with that of  $\text{EuMo}_6\text{S}_8$  slightly larger

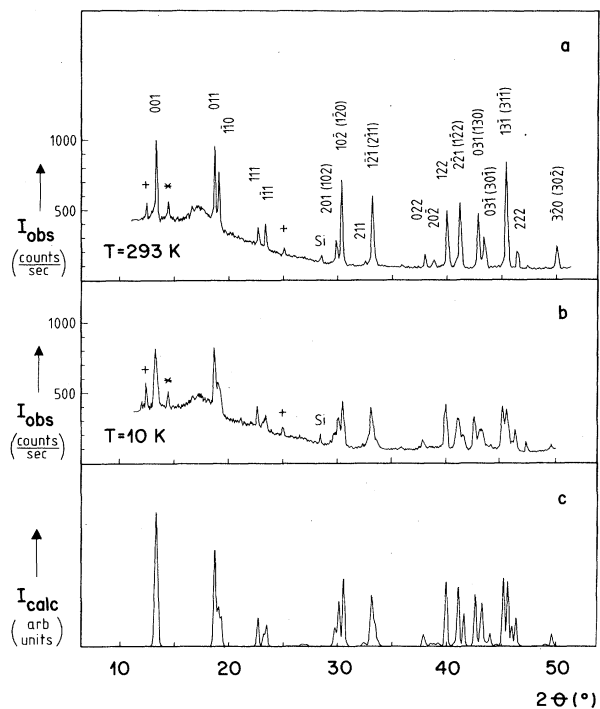


FIG. 2. Same as Fig. 1, for  $\text{BaMo}_6\text{S}_8$ . The lines marked by asterisks and crosses belong, respectively, to  $\text{MoS}_2$  and an unknown phase.

than that of  $\text{BaMo}_6\text{S}_8$ .

Parallel to this study, a single-crystal fragment of  $\text{BaMo}_6\text{S}_8$  was examined on a four-circle diffractometer (Philips PW 1100) which was equipped with a  $\text{N}_2$ -gas low-temperature attachment (Leybold-Heraeus). A study of the lattice parameters as a function of temperature showed that its cell volume remained practically constant (within 0.1%) as the crystal transformed from the rhombohedral high-temperature (HT) into the tri-

TABLE I. Cell parameters for the rhombohedral high-temperature (HT) and the triclinic low-temperature (LT) structures of  $\text{EuMo}_6\text{S}_8$  and  $\text{BaMo}_6\text{S}_8$ .

EuMo <sub>6</sub> S <sub>8</sub> :					
293 K (HT)	$a = 6.565(5) \text{ \AA}$ ,	$\alpha = 88.91(5)^\circ$ ,	$V = 282.8 \text{ \AA}^3$	a	
	$a = 6.53 \text{ \AA}$ ,	$\alpha = 89.3^\circ$ ,	$V = 278.5 \text{ \AA}^3$	(Ref. 1)	
	$a = 6.54 \text{ \AA}$ ,	$\alpha = 89.0^\circ$ ,	$V = 279.0 \text{ \AA}^3$	(Ref. 3)	
10 K (LT)	$a = 6.472(2)$ ,	$b = 6.616(2)$ ,	$c = 6.573(2) \text{ \AA}$ ,	$V = 281.2 \text{ \AA}^3$ <sup>b</sup>	
	$\alpha = 89.26(3)$ ,	$\beta = 88.10(3)$ ,	$\gamma = 89.25(3)^\circ$		
BaMo <sub>6</sub> S <sub>8</sub> :					
293 K (HT)	$a = 6.6483(2) \text{ \AA}$ ,	$\alpha = 88.596(4)^\circ$ ,	$V = 293.6 \text{ \AA}^3$	a	
	$a = 6.64 \text{ \AA}$ ,	$\alpha = 89.0^\circ$ ,	$V = 292.7 \text{ \AA}^3$	(Ref. 1)	
	$a = 6.572(4)$ ,	$b = 6.691(3)$ ,	$c = 6.651(3) \text{ \AA}$ ,	$V = 292.2 \text{ \AA}^3$ <sup>b</sup>	
10 K (LT)	$\alpha = 89.05(4)$ ,	$\beta = 88.10(4)$ ,	$\gamma = 88.90(5)^\circ$		

<sup>a</sup>Single crystal.

<sup>b</sup>Powder.

clinic low-temperature (LT) structure. In order to elucidate the driving mechanism of the phase transformation the atomic parameters were refined for both the HT and LT structures by measuring integrated intensities of 1400 Bragg reflections.<sup>7</sup> The results showed that significant structural changes occurred mainly within the octahedral Mo<sub>6</sub> clusters. During the phase transition their point symmetry was lowered from  $\bar{3}$  to  $\bar{1}$ , i.e., they lost the threefold axis but retained the inversion center. The triclinic distortion changed the Mo-Mo bond lengths by up to 0.03 Å and the Mo-Mo-Mo bond angles by up to 2°. This led to three different Mo-Mo *intercluster* distances [ $d_{\text{Mo-Mo}}^{\text{inter}} = 2 \times 3.42, 2 \times 3.40, 2 \times 3.38$  Å (LT);  $6 \times 3.41$  Å (HT)] and increased the spread of the Mo-Mo *intracluster* distances [ $d_{\text{Mo-Mo}}^{\text{intra}} = 2 \times 2.65, 2 \times 2.65, 2 \times 2.68, 2 \times 2.69, 2 \times 2.69, 2 \times 2.72$  Å (LT);  $6 \times 2.67, 6 \times 2.70$  Å (HT)]. Their average, however, remained practically unchanged [ $\bar{d}_{\text{Mo-Mo}}^{\text{intra}} = 2.682$  Å (LT),  $2.685$  Å (HT)], which indicates that the charge transfer to the Mo<sub>6</sub> clusters<sup>8</sup> and the number of occupied Mo *d*-bonding states is the same in both the HT and LT structures. As can be seen in Fig. 2, the agreement between the observed powder diffraction pattern of triclinic BaMo<sub>6</sub>S<sub>8</sub> at 10 K and a computer-simulated diffraction profile calculated with the atomic parameters at 200 K is excellent.

Because of instrumental limitations, reliable atomic parameters for the LT phase of EuMo<sub>6</sub>S<sub>8</sub> have not been obtained from single-crystal data as yet. In view of the powder diffraction results at 10 K, however, one can assume that its Mo<sub>6</sub> clusters are even more strongly distorted than those of BaMo<sub>6</sub>S<sub>8</sub>, because the triclinic deformation of its lattice is greater. An intensity calculation for triclinic EuMo<sub>6</sub>S<sub>8</sub> using the lattice parameters listed in Table I and the atomic coordinates of triclinic BaMo<sub>6</sub>S<sub>8</sub> (Ref. 7) showed satisfactory agreement between the theoretical and experimental powder patterns [Figs. 1(b) and 1(c)]. Thus one can safely assume that the low-temperature anomalies in the physical properties of EuMo<sub>6</sub>S<sub>8</sub> such as those in resistivity,<sup>5,9</sup> specific heat,<sup>5</sup> and Hall effect<sup>4</sup> are related to the structural phase transformation described above. A possible reason why this transformation has not been detected by x-ray methods before is its subtle nature which leads to only a relatively small distortion of the lattice. Another reason, however, could be related to the different methods of sample preparation. In fact, our BaMo<sub>6</sub>S<sub>8</sub> or Eu<sub>1-x</sub>Mo<sub>6</sub>S<sub>8</sub> samples which were not molten prior

to the low-temperature experiments showed in their x-ray powder patterns only line broadening but no line splitting. They also showed less-pronounced specific heat and resistivity anomalies.<sup>5</sup> The reasons for this difference in behavior between the melted and nonmelted samples are unknown at present.

Structural phase transitions in  $M_x\text{Mo}_6\text{S}_8$  compounds have been observed before. Rhombohedral Cu<sub>1.8</sub>Mo<sub>6</sub>S<sub>8</sub>, for instance, which contains more than one *M* atom per Mo<sub>6</sub>S<sub>8</sub> unit, transforms at 270 K into a triclinic distorted low-temperature variant.<sup>10</sup> The transition is presumably due to an order-disorder transition of the Cu atoms which partially occupy two sets of sixfold equipoints in the HT phase (site symmetry 1) and condense into pairs which occupy only one twofold equipoint in the LT phase (site symmetry 1). The ordering leads to a triclinic deformation of the chalcogen atom network which causes a triclinic distortion of the Mo<sub>6</sub> octahedron. In BaMo<sub>6</sub>S<sub>8</sub> and EuMo<sub>6</sub>S<sub>8</sub>, however, which contain one *M* atom per Mo<sub>6</sub>S<sub>8</sub> unit, there exists only one *M*-atom site of symmetry  $\bar{3}$  in the HT and one of symmetry  $\bar{1}$  in the LT modification.<sup>7</sup> Thus the lowering of the crystal symmetry, and in particular the triclinical deformation of the Mo<sub>6</sub> octahedron, has a different origin. One which appears most likely in view of our structural results is an electronic instability associated with the Mo *d* states. As shown by theoretical band-structure calculations by Andersen, Klose, and Nohl<sup>11</sup> the conduction bands in the rhombohedral *M*Mo<sub>6</sub>S<sub>8</sub> compounds derive mainly from the Mo *d* states of the isolated Mo<sub>6</sub> clusters, and the main conduction band has  $e_g$  symmetry. On the other hand, systematic investigations of their crystal structures have shown that the electronic states of these bands are bonding and contribute significantly to the size and the shape of the Mo<sub>6</sub> octahedra.<sup>8</sup> In electron-rich compounds such as LaMo<sub>6</sub>S<sub>8</sub>, which contains one hole in the conduction bands, the size and the elongation (along  $\bar{3}$ ) of the Mo<sub>6</sub> octahedron are smaller than those of the Mo<sub>6</sub> octahedra in electron-poor compounds such as Mo<sub>6</sub>S<sub>8</sub>, which contains four holes in the conduction bands.<sup>11</sup> In compounds containing divalent metal cations such as Pb<sup>2+</sup> and Sn<sup>2+</sup>, and also Ba<sup>2+</sup> and Eu<sup>2+</sup>, the Mo<sub>6</sub> octahedra have intermediate size and elongation. They carry a formal electric charge of 22 electrons which corresponds to two holes in the conduction bands. Thus, assuming the presence of one conduction band and a compound of perfect stoichiometry the doubly degenerate  $e_g$  band is half filled. This

could lead to a Jahn-Teller-like electronic instability which lifts the degeneracy and thereby lowers the total energy. In view of the bonding character of this band one expects that the  $\text{Mo}_6$  octahedron undergoes a triclinic distortion, such that the shortening of the Mo-Mo *intracluster* bonds corresponds to a localization of the conduction electrons in one of the split subbands. Such a mechanism is consistent with the observed semiconducting behavior of  $\text{EuMo}_6\text{S}_8$  at ambient pressure,<sup>4</sup> and could explain the absence of superconductivity in triclinic  $\text{BaMo}_6\text{S}_8$ . It could perhaps also explain the onset of superconductivity in  $\text{EuMo}_6\text{S}_8$  at high pressure,<sup>3,4</sup> because the rhombohedral to triclinic lattice transformation could be suppressed by the application of hydrostatic pressure. If this is true one expects that  $\text{BaMo}_6\text{S}_8$  also becomes superconducting under pressure. Its critical temperature could be even higher than that of  $\text{EuMo}_6\text{S}_8$  because its  $\text{Mo}_6$  clusters are further apart from each other [ $d_{\text{Mo-Mo}}^{\text{inter}} = 3.27 \text{ \AA}$ ,  $d_{\text{Mo-S}}^{\text{inter}} = 2.58 \text{ \AA}$  (HT  $\text{EuMo}_6\text{S}_8$ );  $d_{\text{Mo-Mo}}^{\text{inter}} = 3.41 \text{ \AA}$ ,  $d_{\text{Mo-S}}^{\text{inter}} = 2.62 \text{ \AA}$  (HT  $\text{BaMo}_6\text{S}_8$ )]<sup>7</sup> and thus its conduction bands are narrower.<sup>11</sup>

We are grateful to P. Fischer from Eidgenössisches Institut für Reaktorforschung, Würenlingen, for his help in the computer simulation of

the x-ray powder diffraction profiles.

<sup>(a)</sup>Département de Physique de la Matière Condensée.

<sup>(b)</sup>Laboratoire de Cristallographie aux Rayons X.

<sup>1</sup>Ø. Fischer, Appl. Phys. **16**, 1 (1978).

<sup>2</sup>T. Jarlborg and A. J. Freeman, Phys. Rev. Lett. **44**, 178 (1980).

<sup>3</sup>C. W. Chu, S. Z. Hunag, C. H. Lin, R. L. Meng, M. K. Wu, and P. H. Schmidt, Phys. Rev. Lett. **46**, 276 (1981).

<sup>4</sup>D. W. Harrison, K. C. Lim, J. D. Thompson, C. Y. Huang, P. D. Hamburger, and H. L. Luo, Phys. Rev. Lett. **46**, 280 (1981).

<sup>5</sup>R. Baillif, A. Junod, B. Lachal, J. Muller, and K. Yvon, to be published.

<sup>6</sup>K. Yvon, W. Jeitschko, and E. Parthé, J. Appl. Crystallogr. **10**, 73 (1977).

<sup>7</sup>A. Dunand, R. Baillif, and K. Yvon, to be published.

<sup>8</sup>K. Yvon, in *Current Topics in Materials Science*, edited by K. Kaldis (North-Holland, Amsterdam, 1979), Vol. 3.

<sup>9</sup>M. B. Maple, L. E. DeLong, W. A. Fertig, D. C. Johnston, R. W. McCallum, and R. N. Shelton, in *Valence Instabilities and Related Narrow Band Phenomena*, edited by R. D. Parks (Plenum, New York, 1977), p. 17.

<sup>10</sup>R. Baillif, K. Yvon, R. Flükiger, and J. Muller, J. Low Temp. Phys. **37**, 231 (1979).

<sup>11</sup>O. K. Andersen, W. Klose, and H. Nohl, Phys. Rev. B **17**, 1209 (1978).

## Universal Binding Energy Curves for Metals and Bimetallic Interfaces

J. H. Rose

Ames Laboratory, Iowa State University, Ames, Iowa 50011

and

John Ferrante

National Aeronautics and Space Administration, Lewis Research Center, Cleveland, Ohio 44135

and

John R. Smith

Physics Department, General Motors Research Laboratories, Warren, Michigan 48090

(Received 27 April 1981)

We provide evidence for a universal relationship between metallic binding energies and lattice parameters. By a simple scaling of a universal relationship, one can obtain binding energies as a function of atomic separation for bimetallic interfaces and bulk metals.

PACS numbers: 61.50.Lt

Solid-state energetics are fundamentally described by the relation between the total energy and an appropriate atomic separation. Equations of state, reaction kinetics, and relative atomic configurations are examples of quantities which

depend sensitively on the energy as a function of separation. Such energy-distance relations cannot be obtained for solids with use of modern experimental techniques. They can, however, be determined by *ab initio* calculations. However,